Two Distinct N-Glycosylation Pathways Process the *Haloferax volcanii* S-Layer Glycoprotein upon Changes in Environmental Salinity

Lina Kaminski,[a] Ziqiang Guan,[b] Sophie Yurist-Doutsch,[a]* Jerry Eichler[a]

Department of Life Sciences, Ben Gurion University of the Negev, Beersheva, Israel[a]; Department of Biochemistry, Duke University Medical Center, Durham, North Carolina, USA[b]

* Present address: Sophie Yurist-Doutsch, Michael Smith Laboratories, University of British Columbia, Vancouver, BC, Canada.

ABSTRACT **N-glycosylation in *Archaea* presents aspects of this posttranslational modification not seen in either *Eukarya* or *Bacteria*. In the haloarchaeon *Haloferax volcanii*, the surface (S)-layer glycoprotein can be simultaneously modified by two different N-glycans. Asn-13 and Asn-83 are modified by a pentasaccharide, whereas Asn-498 is modified by a tetrasaccharide of distinct composition, with N-glycosylation at this position being related to environmental conditions. Specifically, N-glycosylation of Asn-498 is detected when cells are grown in the presence of 1.75 but not 3.4 M NaCl. While deletion of genes encoding components of the pentasaccharide assembly pathway had no effect on the biosynthesis of the tetrasaccharide bound to Asn-498, deletion of genes within the cluster spanning *HVO_2046* to *HVO_2061* interfered with the assembly and attachment of the Asn-498-linked tetrasaccharide. Transfer of the "low-salt" tetrasaccharide from the dolichol phosphate carrier upon which it is assembled to S-layer glycoprotein Asn-498 did not require AglB, the oligosaccharyltransferase responsible for pentasaccharide attachment to Asn-13 and Asn-83. Finally, although biogenesis of the low-salt tetrasaccharide is barely discernible upon growth at the elevated salinity, this glycan was readily detected under such conditions in strains deleted of pentasaccharide biosynthesis pathway genes, indicative of cross talk between the two N-glycosylation pathways.**

IMPORTANCE **In the haloarchaeon *Haloferax volcanii*, originally from the Dead Sea, the pathway responsible for the assembly and attachment of a pentasaccharide to the S-layer glycoprotein, a well-studied glycoprotein in this species, has been described. More recently, it was shown that in response to growth in low salinity, the same glycoprotein is modified by a novel tetrasaccharide. In the present study, numerous components of the pathway used to synthesize this "low-salt" tetrasaccharide are described. As such, this represents the first report of two N-glycosylation pathways able to simultaneously modify a single protein as a function of environmental salinity. Moreover, and to the best of our knowledge, the ability to N-glycosylate the same protein with different and unrelated glycans has not been observed in either *Eukarya* or *Bacteria* or indeed beyond the halophilic archaea, for which similar dual modification of the *Halobacterium salinarum* S-layer glycoprotein was reported.**

Received 28 August 2013 **Accepted** 10 October 2013 **Published** 5 November 2013

Citation Kaminski L, Guan Z, Yurist-Doutsch S, Eichler J. 2013. Two distinct N-glycosylation pathways process the *Haloferax volcanii* S-layer glycoprotein upon changes in environmental salinity. mBio 4(6):e00716-13. doi:10.1128/mBio.00716-13.

Invited Editor Maria Hadjifrangiskou, Vanderbilt University School of Medicine **Editor** Scott Hultgren, Washington University School of Medicine

Address correspondence to Jerry Eichler, jeichler@bgu.ac.il.

N-glycosylation, the covalent attachment of glycans to select asparagine residues of target proteins, is a posttranslational modification performed by members of all three domains of life (1–5). N-glycosylation in *Archaea*, although seemingly common (6) and involving a diversity of sugars not seen elsewhere (4, 5), nonetheless remains less well understood than the parallel eukaryal and bacterial systems. Of late, however, a series of genetic and biochemical studies of *Haloferax* (*Hfx.*) *volcanii* (see reference 5) and other species (7–12) have begun to provide insight into the archaeal version of this universal protein-processing event.

In *Hfx. volcanii*, the surface (S)-layer glycoprotein, a well-studied glycoprotein and sole component of the protein shell surrounding cells of this species, is modified by a pentasaccharide comprising a hexose, two hexuronic acids, a methyl ester of hexuronic acid, and a mannose (13, 14) via the actions of a series of Agl (*a*rchaeal *gl*ycosylation) proteins. Here, the glycosyltransferases AglJ, AglG, AglI, and AlgE sequentially add the first four sugars of the pentasaccharide to a common dolichol phosphate (DolP) carrier (15–18). Once the lipid-linked tetrasaccharide (and its precursors) is translocated across the plasma membrane, the glycan is N-linked to the S-layer glycoprotein by the oligosaccharyltransferase (OST) AglB (13). The final sugar of the N-linked pentasaccharide, mannose, is added to its own DolP carrier on the cytoplasmic face of the membrane by AglD, translocated to face the cell exterior in a process involving AglR, and then transferred to the protein-linked tetrasaccharide by AglS (17, 19–22). Finally, other Agl proteins, such as AglF, AglM, and AglP, also contribute to pentasaccharide assembly, serving various sugar-processing roles (14–23).

Hfx. volcanii, first isolated from the Dead Sea (24), requires molar concentrations of salt for survival. Recently, it was reported that N-glycosylation of the S-layer glycoprotein, in direct contact

with the hypersaline surroundings in which such cells exist, changes as a function of environmental salinity (25). S-layer glycoproteins Asn-13 and Asn-83 bear the pentasaccharide described above in cells raised in either 1.75 M or 3.4 M NaCl-containing growth medium, although such modification is substantially reduced upon growth at the lower salinity. More strikingly, S-layer glycoprotein Asn-498, whose position is not modified in cells grown at the higher salinity, is modified by a novel tetrasaccharide comprising a sulfated hexose, two hexoses, and a rhamnose in cells grown at the lower salt concentration. The modulation of the S-layer glycoprotein N-glycosylation profile in response to changing environmental conditions represents a novel role for this common posttranslational modification.

To the best of our knowledge, the ability to N-glycosylate the same protein with different and unrelated glycans has not been observed in either *Eukarya* or *Bacteria* or indeed beyond the halophilic archaea, for which similar dual modification of the *Halobacterium* (*Hbt.*) *salinarum* S-layer glycoprotein was previously reported (26). Still, it is not known whether the Agl pathway, responsible for the assembly and attachment of the pentasaccharide bound at the *Hfx. volcanii* S-layer glycoprotein Asn-13 and Asn-83 positions, is also involved in generating the "low-salt" tetrasaccharide bound to Asn-498 or whether a novel N-glycosylation pathway is responsible. In the present study, this was addressed.

RESULTS

Assembly of the S-layer glycoprotein Asn-13- and Asn-83-linked pentasaccharide and the Asn-498-linked low-salt tetrasaccharide rely on different pathways. To determine whether the same Agl pathway responsible for generating the pentasaccharide N-linked to S-layer glycoprotein Asn-13 and Asn-83 (13, 14) is also responsible for generating the low-salt tetrasaccharide bound to Asn-498 (25), N-glycosylation at this position was considered in *Hfx. volcanii* cells lacking AglI or AglE, glycosyltransferases involved in pentasaccharide assembly (15, 16), and grown in 1.75 M NaCl-containing (low-salt) medium. These mutants were selected for such analysis, as the shortened N-linked glycan decorating Asn-13 and Asn-83 in each case is readily detected by mass spectrometry.

To assess the contributions of AglI and AglE to Asn-498 glycosylation, liquid chromatography-electrospray ionization mass spectrometry (LC-ESI MS) was employed. Initially, the LC-ESI MS profile of an S-layer glycoprotein-derived Asn-83-containing peptide generated by trypsin and Glu-C protease treatment (^{65}NQPLGTYDVDGSGSATTPNVTLLAPR^{90}) from Δ*aglI* cells grown in low-salt medium was considered. Whereas no peptide modified by the first three pentasaccharide sugars (*m/z* 1,597.675, calculated $[M + 2H]^{2+}$ mass) was detected (Fig. 1A, top, left), a peptide modified by the first two pentasaccharide sugars, a hexose and a hexuronic acid, was observed ($[M + 2H]^{2+}$ peak at *m/z* 1,491.70) (Fig. 1A, top, right). These results reflect the previously reported role of AglI in adding the third pentasaccharide sugar, a hexuronic acid, to disaccharide-charged DolP, from where it is transferred to S-layer glycoprotein Asn-83 (16). At the same time, when a total lipid extract of the Δ*aglI* cells grown in low-salt medium was examined, $[M-2H]^{2-}$ peaks at *m/z* 780.457 and 814.479, corresponding to C_{55} and C_{60} DolPs modified by a sulfated hexose, two hexoses, and a rhamnose, namely, the complete low-salt tetrasaccharide (25), were observed (Fig. 1A, middle). The same low-salt tetrasaccharide was also detected when an S-layer glycoprotein-derived Asn-498-containing peptide (^{497}INGTAS GANSVLVIFVD^{513}; calculated $[M + 2H]^{2+}$ mass, 1,675.88 Da) from cells lacking AglI grown in low-salt medium was examined by LC-ESI MS. The resulting profile included an *m/z* 1,195.03 peak (Fig. 1A, bottom), as well as *m/z* 1,122.01, 1,040.97, and 959.95 peaks (see Fig. S1 in the supplemental material, left column). These values are in good agreement with, respectively, the predicted $[M + 2H]^{2+}$ values of the Asn-498-containing peptide modified by the complete low-salt tetrasaccharide (*m/z* 1,194.94) and precursors comprising the first three (*m/z* 1,121.94), the first two (*m/z* 1,040.94), and the first (*m/z* 959.94) sugar components of this glycan (25). Likewise, in keeping with the role of AglE in adding the fourth pentasaccharide sugar, a hexuronic acid that is subsequently methylated by AglP (14, 15), the LC-ESI MS profile of proteolytic S-layer glycoprotein fragments from cells lacking AglE did not present a peak corresponding to the Asn-83-containing peptide modified by the first four pentasaccharide sugars (*m/z* 1,674.675, calculated $[M + 2H]^{2+}$ mass) (Fig. 1B, top, left). Instead, an $[M + 2H]^{2+}$ peak at *m/z* 1,579.72, corresponding to the same peptide modified by the first three sugars of the Asn-83-bound pentasaccharide was seen (Fig. 1B, top, right). LC-ESI MS analysis of a total lipid extract of the same cells revealed $[M-2H]^{2-}$ peaks at *m/z* 780.448 and 814.475, corresponding to C_{55} and C_{60} DolPs modified by the low-salt tetrasaccharide, respectively (Fig. 1B, middle). At the same time, the LC-ESI MS profile of the Asn-498-containing peptide from such cells presented $[M + 2H]^{2+}$ peaks at *m/z* 1,195.04 (Fig. 1B, bottom), 1,122.03, and 1,040.97 (Fig. S1, right column), respectively, corresponding to the low-salt tetrasaccharide and its tri- and disaccharide precursors.

These observations thus point to the assembly of the low-salt tetrasaccharide bound to S-layer glycoprotein Asn-498 as relying on a biosynthetic pathway distinct from that used for assembly of the pentasaccharide that modifies the Asn-13 and Asn-83 positions.

A novel N-glycosylation pathway modifies S-layer glycoprotein Asn-498. Apart from *aglD*, all of the *Hfx. volcanii* genes involved in the assembly of the N-linked pentasaccharide decorating S-layer glycoprotein Asn-13 and Asn-83 are organized into a single cluster spanning *HVO_1517* (*aglJ*) to *HVO_1531* (*aglM*) (16, 27). To begin identifying components of the novel pathway involved in assembly of the low-salt tetrasaccharide, the *Hfx. volcanii* genome sequence (28) was scanned for other clusters of open reading frames (ORFs) annotated as serving glycosylation-related roles. ORFs comprising the region spanning from *HVO_2046* to *HVO_2061* represents one such region. Table S1 in the supplemental material summarizes the current annotations of these sequences, as well as the predicted subcellular localization of the deduced products.

The participation of genes within the *HVO_2046-2061* region in generating the low-salt tetrasaccharide bound to Asn-498 was next considered by deleting each sequence within the cluster and assessing the effects of such deletion on Asn-498 glycosylation. The various deletion strains were generated by the "pop-in/pop-out" technique developed for use with *Hfx. volcanii*, in which the *trpA* gene, encoding tryptophan synthase, is introduced into a strain auxotrophic for tryptophan in place of the gene being deleted (29). In each case, deletion was confirmed (Fig. S2) and the effect of each deletion was assessed by LC-ESI MS both at the level

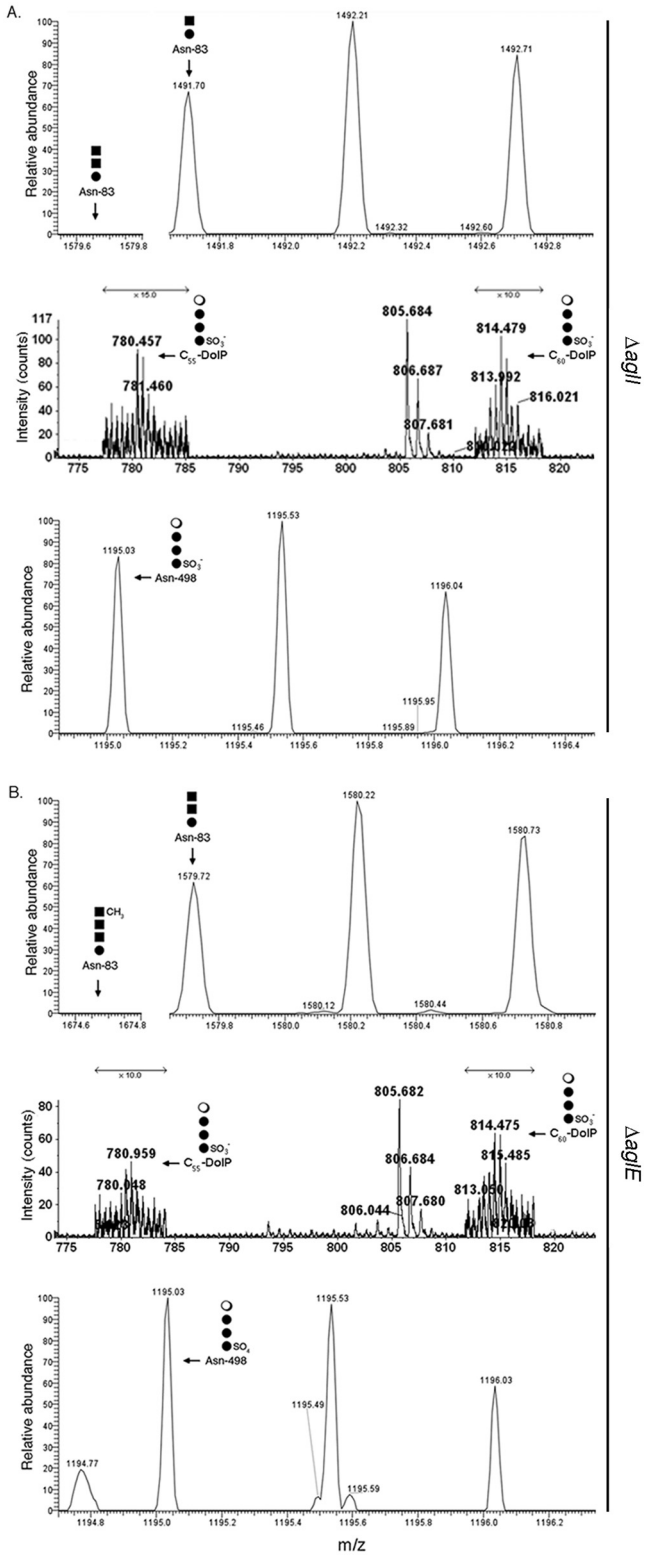

FIG 1 The Agl pathway is not involved in biogenesis of the low-salt tetrasaccharide. In Δ*aglI* and Δ*aglE* cells grown in low-salt medium, S-layer glycoprotein Asn-498 is modified by the low-salt tetrasaccharide. LC-ESI MS profiles of S-layer glycoprotein-derived peptides containing Asn-83 (top) or Asn-498 (bottom) or of total lipid extracts (middle) from Δ*aglI* (A) and Δ*aglE* (B) cells. In each peptide-derived profile, arrows point to monoisotopic $[M + 2H]^{2+}$ ion peaks corresponding to glycan-modified peptides or their expected

(Continued)

of the DolP carrier upon which the low-salt tetrasaccharide is assembled (25) and at the level of S-layer glycoprotein Asn-498.

In the case of Δ*HVO_2058* cells, analysis of the LC-ESI MS profile of a total lipid extract revealed C_{55} and C_{60} DolPs modified by the first three sugars of the low-salt tetrasaccharide ($[M\text{-}2H]^{2-}$ ion peaks at *m/z* 707.415 and 741.443, respectively) (Fig. 2A, left) but not by the complete tetrasaccharide (Fig. 2A, right). Likewise, when the Asn-498-containing S-layer glycoprotein-derived peptide from the same cells grown in low-salt medium was analyzed, a $[M + 2H]^{2+}$ ion peak at *m/z* 1,122.03 was observed, corresponding to the peptide modified by the trisaccharide precursor of the low-salt tetrasaccharide (Fig. 2B, upper). No peptide modified by the complete tetrasaccharide was detected (Fig. 2B, lower). HVO_2058 is thus involved in the addition of rhamnose onto DolP charged with the first three sugars of the low-salt tetrasaccharide. To confirm that the effect of *HVO_2058* deletion on low-salt tetrasaccharide biogenesis was not due to a downstream effect, cells of the deletion strain were transformed to express a plasmid-derived version of the protein bearing a *Clostridium thermocellum* cellulose-binding domain (CBD) tag. The transformed strain was able to assemble and attached the complete low-salt tetrasaccharide to S-layer glycoprotein Asn-498 (Fig. 2C). Finally, to gain insight into *HVO_2058* transcription as a function of growth medium salinity, quantitative PCR was performed. Relative to the level of *HVO_2058* transcript measured in cells grown in 3.4 M NaCl-containing medium, 0.75-fold (±0.22-fold, standard deviation, $n = 5$) the transcript was seen in cells grown in 1.75 M NaCl-containing medium. As such, comparable levels of the *HVO_2058* transcript are found at the different levels of salinity.

At the same time, C_{55} and C_{60} DolPs in Δ*HVO_2048* cells were modified by only the first two sugars of the low-salt tetrasaccharide ($[M\text{-}2H]^{2-}$ ion peaks at *m/z* 626.382 and 660.408) (Fig. S3A, left); no peaks corresponding to the same lipids bearing the first three sugars of the low-salt tetrasaccharide were detected (Fig. S3A, right). Analysis of the Asn-498-containing peptide from these cells revealed a $[M + 2H]^{2+}$ ion peak of *m/z* 1,040.97 (Fig. S3B, upper), corresponding to the peptide modified by the first two sugars of the low-salt tetrasaccharide; no peptide modified by the trisaccharide precursor of the Asn-498-linked low-salt tetrasaccharide was observed (Fig. S3B, lower). As such, it can be concluded that HVO_2048 is involved in the addition of the third sugar of the low-salt tetrasaccharide to DolP. To assess the effects of growth medium salinity on *HVO_2048* transcription, quantitative PCR was performed. Relative to the level of *HVO_2048* transcript measured in cells grown in 3.4 M NaCl-containing medium, 0.76-fold (±0.44-fold, standard deviation, $n = 5$) of the transcript was seen in cells grown in 1.75 M NaCl-containing medium. It thus appears that the level of *HVO_2048* transcription does not change substantially as a function of medium salinity.

Using the same experimental strategy, roles for HVO_2046, HVO_2049, HVO_2053, HVO_2055, HVO_2056, HVO_2057,

Figure Legend Continued

positions, while in the lipid-derived profiles, arrows point to monoisotopic $[M\text{-}2H]^{2-}$ ion peaks corresponding to low-salt tetrasaccharide-modified DolP. Adjacent to each arrow is a schematic depiction of the Asn- or DolP-bound glycan detected (or not), with the filled circles corresponding to hexose, the filled squares corresponding to hexuronic acid, and the open circle corresponding to rhamnose. In the middle panels, the arrows indicating ×10 reflect magnification of the ion peaks in the corresponding region of the profile.

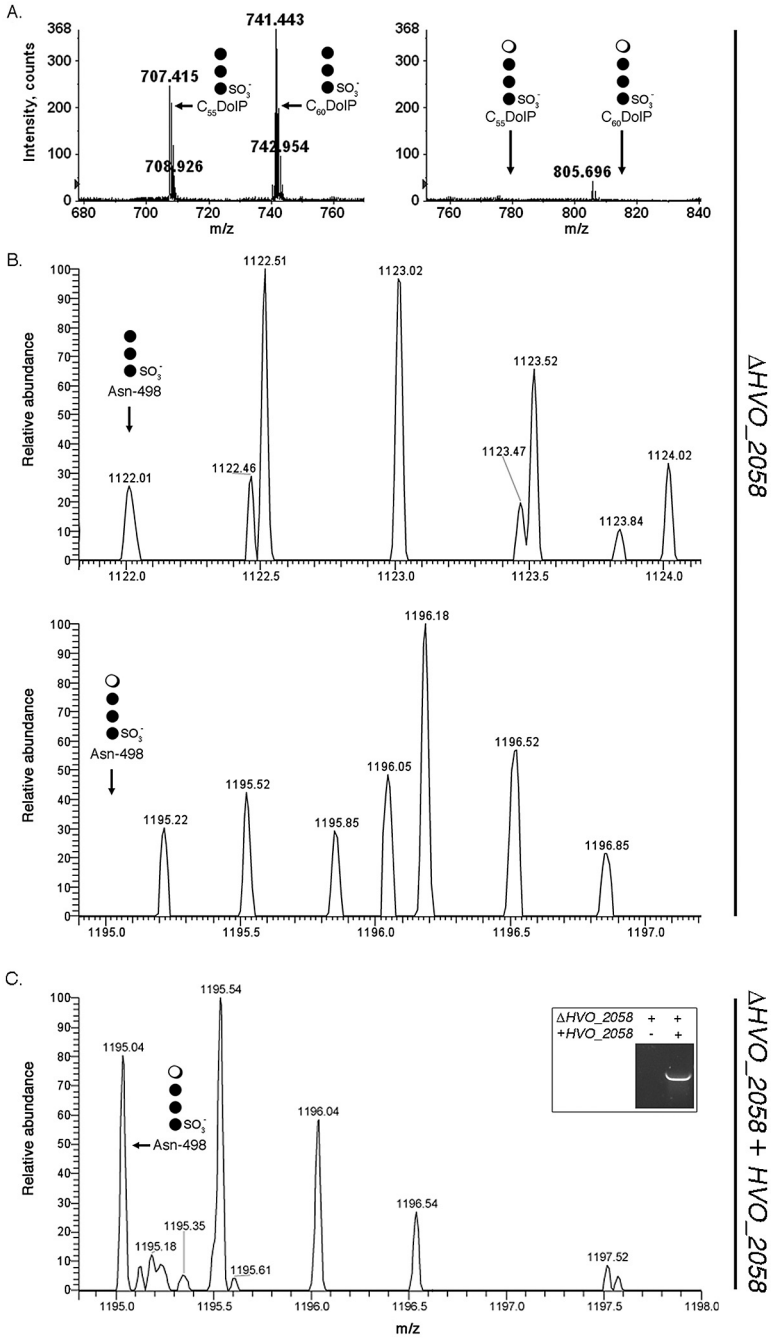

FIG 2 Deletion of *HVO_2058* affects DolP and Asn-498 glycosylation. (A) In cells lacking HVO_2058, C_{55} and C_{60} DolPs are modified by the first three sugars of the complete low-salt tetrasaccharide (left) but not by the complete glycan (right). (B) The S-layer glycoprotein-derived Asn-498-containing peptide from Δ*HVO_2058* cells is modified by the first three sugars of the low-salt tetrasaccharide (upper) but not by the complete glycan (lower). (C) In cells of the deletion strain transformed with plasmid pWL-CBD2058, encoding a CBD-tagged version of HVO_2058, the S-layer glycoprotein-derived Asn-498-containing peptide is modified by the complete low-salt tetrasaccharide. The inset shows PCR amplification of *CBD-HVO_2058* in the transformed strain but not in the deletion strain. In each panel in the figure, the position of each detected or absent glycan-modified DolP or Asn-498-containing peptide is indicated, as is a schematically drawn depiction of the present or absent glycan. In the schematic drawings, the open circle represents rhamnose, while the filled circles represent hexose.

HVO_2059, HVO_2060, and HVO_2061 in *Hfx. volcanii* S-layer glycoprotein Asn-498 glycosylation were also revealed (Table 1). In the case of HVO_2047, deletion of the encoding gene did not reveal any effect on the low-salt tetrasaccharide at either the DolP or the S-layer glycoprotein level. As such, either HVO_2047 is not involved in N-glycosylation, as related to the low-salt tetrasaccharide, or it mediates an effect not revealed by the mass spectrometry-based analysis employed, as, for example, would be the case for an epimerase.

Given the roles of products of genes in the *HVO_2046-2061* region in the biogenesis of the low-salt tetrasaccharide, these were renamed Agl5 (HVO_2053), Agl6 (HVO_2061), Agl7

TABLE 1 Genes involved in the biogenesis of the low-salt tetrasaccharide[a]

Deletion (gene designation)	C_{55} or C_{60}-DolP species observed	S-layer glycoprotein Asn-498 glycosylation
ΔHVO_2046 (*agl7*)	DolP-●●●○	N_{498}-●
ΔHVO_2048 (*agl9*)	DolP-●SO_3-●	N_{498}-●SO_3- ●
ΔHVO_2049 (*agl10*)	DolP-●SO_3-●●	N_{498}-●SO_3- ●●
ΔHVO_2053 (*agl5*)	DolP-●	Not observed
ΔHVO_2055 (*agl15*)	DolP-●SO_3-●●○	Not observed
ΔHVO_2056 (*agl13*)	DolP-●SO_3-●●	N_{498}-●SO_3- ●●
ΔHVO_2057 (*agl11*)	DolP-●SO_3-●●	N_{498}-●SO_3- ●●
ΔHVO_2058 (*agl14*)	DolP-●SO_3-●●	N_{498}-●SO_3- ●●
ΔHVO_2059 (*agl12*)	DolP-●SO_3-●●	N_{498}-●SO_3- ●●
ΔHVO_2060 (*agl8*)	DolP-●SO_3-●	N_{498}-●SO_3- ●
ΔHVO_2061 (*agl6*)	DolP-●	Not observed

[a] Filled circles represent hexose, and the open circles represent rhamnose.

(HVO_2046), Agl8 (HVO_2060), Agl9 (HVO_2048), Agl10 (HVO_2049), Agl11 (HVO_2057), Agl12 (HVO_2059), Agl13 (HVO_2056), Agl14 (HVO_2058), and Agl15 (HVO_2055), according to the nomenclature for archaeal N-glycosylation pathway components first proposed by Chaban et al. (7) and recently expanded by Meyer et al. (10) (for further discussion, see reference 30). Finally, the absence of Agl5-Agl15 did not compromise Asn-13 and Asn-83 glycosylation (Fig. S4), reflecting the specific contributions of these proteins to the assembly of the low-salt tetrasaccharide.

The oligosaccharyltransferase AglB is not needed for Asn-498 glycosylation. Although *Hfx. volcanii* seemingly relies on two different pathways for the assembly of the two N-linked glycans decorating the S-layer glycoprotein, only one oligosaccharyltransferase, AglB, has been identified in this organism (6, 31). In agreement with earlier studies (13), an S-layer glycoprotein-derived Asn-83-containing peptide ($[M + 2H]^{2+}$ ion peak at *m/z* 1,322.66) (Fig. 3A, upper) was not modified in cells deleted of *aglB* (Fig. 3A, lower). Next, to determine whether AglB also catalyzes transfer of the low-salt tetrasaccharide from DolP to Asn-498, Δ*aglB* cells were grown in low-salt medium and modification of the S-layer glycoprotein was considered by LC-ESI MS. Analysis of the S-layer glycoprotein-derived Asn-498-containing peptide revealed peaks corresponding to the peptide modified by the complete low-salt tetrasaccharide ($[M + 2H]^{2+}$ ion peak at *m/z* 1,195.04) (Fig. 3B), as well as by the first ($[M + 2H]^{2+}$ ion peak at *m/z* 959.96) (Fig. S5, top), the first two ($[M + 2H]^{2+}$ ion peak at *m/z* 1,040.97) (Fig. S5, middle), and the first three ($[M + 2H]^{2+}$ ion peak at *m/z* 1,122.02) (Fig. S5, bottom) low-salt tetrasaccharide sugars. It thus appears that AglB is not involved in the transfer of the low-salt tetrasaccharide from its DolP carrier to S-layer glycoprotein Asn-498.

When grown in high salt, cells lacking glycosyltransferases involved in Asn-13 and Asn-83 glycosylation decorate Asn-498 with the low-salt tetrasaccharide. Finally, experiments were undertaken to assess whether interplay between the two *Hfx. volcanii* N-glycosylation pathways exists. Specifically, it was tested whether the pathway responsible for biosynthesis of the low-salt tetrasaccharide could decorate Asn-498 in cells grown in medium containing 3.4 M NaCl when components of the pathway responsible for the assembly of the pentasaccharide N-linked to S-layer glycoprotein Asn-13 and Asn-83 were missing. Accordingly, N-glycosylation of Asn-498 was considered in cells deleted of *aglI* or *aglE* and grown in high-salt medium.

As previously reported (25), cells of the parent strain grown in high-salt medium contained barely detectable amounts of C_{55} and C_{60} DolPs modified by the low-salt tetrasaccharide ($[M-2H]^{2-}$ ion peaks detected at *m/z* 780.465 and 814.484, respectively) (Fig. 4A, inset). As expected, no low-salt tetrasaccharide was linked to S-layer glycoprotein Asn-498 in parent strain cells raised at the higher salinity (4A). When, however, the glycan-charged pools of DolP from cells deleted of *aglI* or *aglE* and grown in 3.4 M NaCl were examined, considerably more low-salt tetrasaccharide-charged DolP was detected than in the parent strain, with the unrelated *m/z* 805.7 peak serving as an internal control in each case (upper panels, Fig. 4B and Fig. S6, respectively). At the same time, analysis of the S-layer glycoprotein-derived peptides obtained from cells lacking AglI (Fig. 4B, bottom) or AglE (Fig. S6, bottom) and grown in high-salt medium revealed that low-salt tetrasaccharide-modified Asn-498-containing peptide was readily detected.

DISCUSSION

In *Hfx. volcanii* and in *Hbt. salinarum*, glycoproteins can be simultaneously modified by two distinct N-linked glycans, each attached via a different linking sugar (25, 26). Such complexity in N-glycosylation has not been reported beyond these two archaeal species. However, unlike *Hbt. salinarum*, where the pathway(s) of N-glycosylation has not yet been characterized, much is known of the parallel process in *Hfx. volcanii*. In the present study, efforts were directed at determining whether the same pathway employed for generating the pentasaccharide N-linked to *Hfx. volcanii* S-layer glycoprotein Asn-13 and Asn-83 (13, 14) is also responsible for the assembly and attachment of the low-salt tetrasaccharide N-linked to Asn-498 (25) of the same protein when the cells are grown in low-salt medium.

Gene deletions, combined with mass spectrometric analysis of glycan-charged DolP and the S-layer glycoprotein, revealed that Agl proteins involved in the assembly of the Asn-13- and Asn-83-linked pentasaccharide do not participate in the biosynthesis of the low-salt tetrasaccharide attached to Asn-498. Instead, the products of a distinct set of genes mediate the assembly and attachment of this glycan. Given the substantial differences in the compositions of the two N-linked glycans decorating the S-layer glycoprotein, it is not surprising that two distinct assembly pathways are involved. On the other hand, the finding that the OST AglB is not needed for low-salt tetrasaccharide attachment to S-layer glycoprotein Asn-498 is unexpected, as AglB is essential for N-glycosylation of Asn-13 and Asn-83 in cells grown in either high-salt or low-salt medium. In *Hfx. volcanii*, and indeed in *Hbt.*

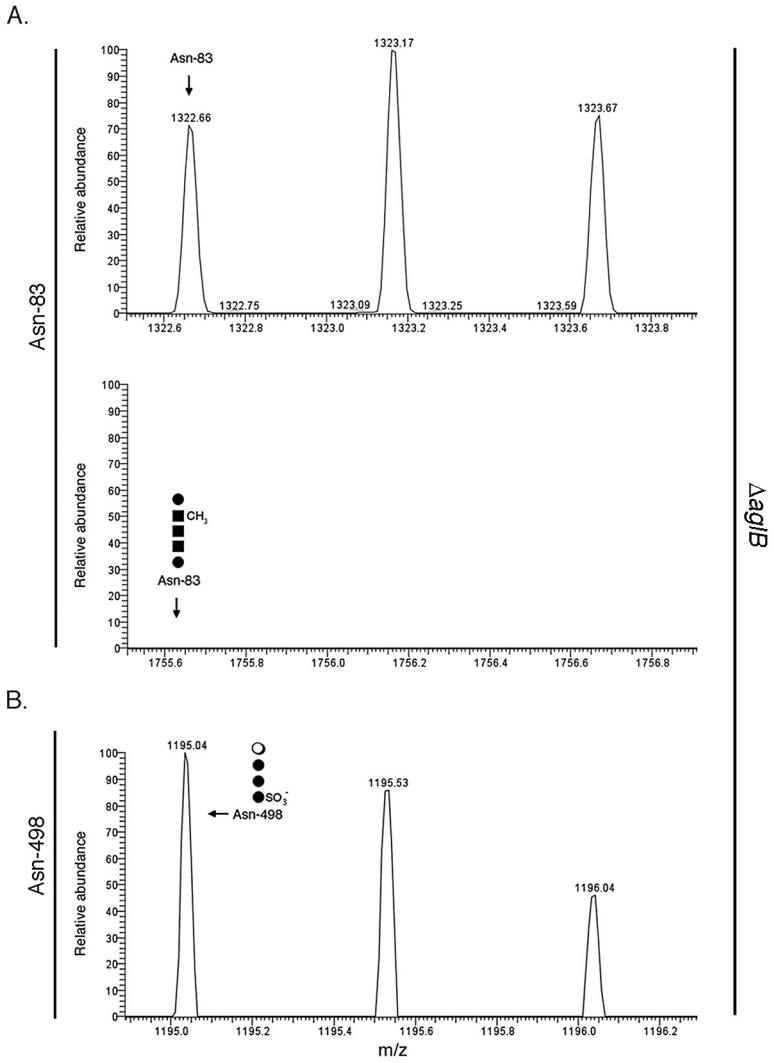

FIG 3 AglB is not involved in S-layer glycoprotein Asn-498 glycosylation. (A) Δ*aglB* cells were grown in low-salt medium. LC-ESI MS analysis reveals the unmodified Asn-83-containing S-layer glycoprotein-derived peptide (upper) but not the same peptide modified by the normally bound pentasaccharide (lower). (B) LC-ESI MS analysis of the S-layer glycoprotein-derived Asn-498-containing peptide from cells lacking AglB reveals modification by the low-salt tetrasaccharide. In each panel, the position of the Asn-83 (A)- or Asn-498 (B)-containing peptide (detected or absent) is indicated, as is a schematically drawn depiction of the present or absent glycan. In the schematic drawings, the filled circles represent hexose, the filled squares represent hexuronic acid, and the open circle represents rhamnose.

salinarum, a single version of AglB is the only homologue of the eukaryal OST catalytic subunit, Stt3, or the bacterial OST, PglB, detected (6, 32). As such, a currently unidentified OST is involved in the delivery of the low-salt tetrasaccharide (and its precursors) from DolP to S-layer glycoprotein Asn-498. The same may well hold true in *Hbt. salinarum*, where one N-linked glycan is transferred from a dolichol phosphate carrier and the second from a dolichol pyrophosphate carrier (26, 33).

Based on the effects of deleting *agl5-agl15* on DolP and S-layer glycoprotein glycosylation, a preliminary pathway for low-salt tetrasaccharide biogenesis can be drawn (Fig. 5). In this working model, Agl5 and Agl6 are assigned roles in adding the linking hexose to DolP, while Agl7 contributes to the sulfation of this lipid-linked sugar. As such, the DolP-hexose seen in cells lacking Agl5 or Agl6 may correspond to this lipid charged with the first sugar of the pentasaccharide transferred to Asn-13 and Asn-83, a process that also occurs under low-salt conditions (25). Moreover, because cells lacking Agl7 contained DolP charged with a nonsulfated version of the low-salt tetrasaccharide, while no Asn-498-fused low-salt tetrasaccharide (or its di- or trisaccharide precursors) were detected, sulfation of the DolP-bound hexose may be needed for translocation of DolP charged with a more elaborate precursor of the low-salt tetrasaccharide or the complete glycan across the plasma membrane. Further work will be required to define the precise actions of Agl5, Agl6, and Agl7, as well as the order in which they act. Agl8 and Agl9 contribute to the addition of a hexose to disaccharide-charged DolP. Similarly, Agl10 to Agl14 are involved in the appearance of the final rhamnose sugar of the low-salt tetrasaccharide on the DolP carrier. In contrast, cells lacking Agl15 assemble the intact low-salt tetrasaccharide on DolP, yet no such glycan is observed on S-layer glycoprotein Asn-498. This effect is consistent with Agl15 acting as a flippase, medi-

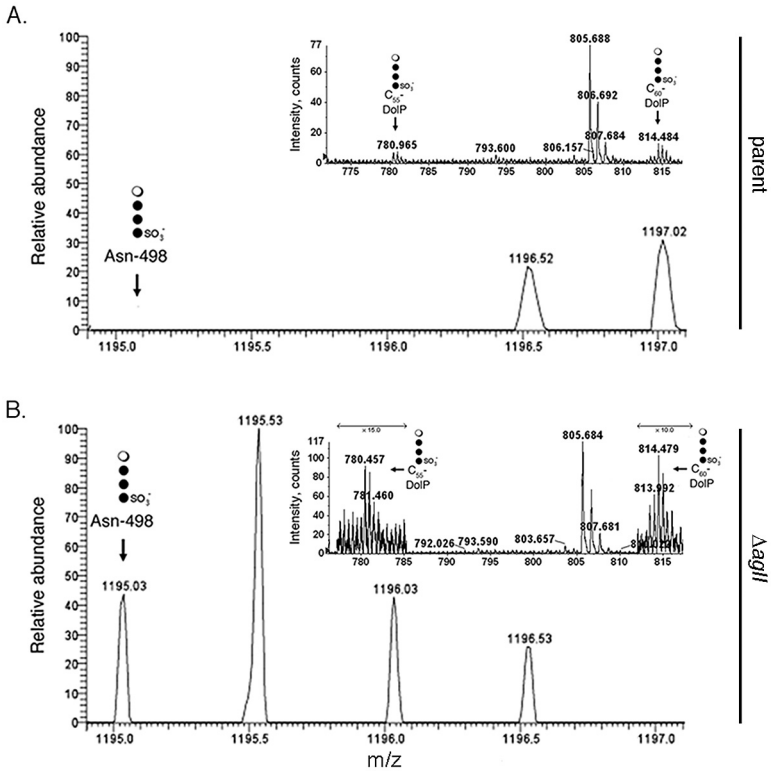

FIG 4 *Hfx. volcanii* Δ*aglI* cells grown in 3.4 M NaCl-containing growth medium modify DolP and S-layer glycoprotein Asn-498 with the low-salt tetrasaccharide. (A) In parent strain cells, no Asn-498-containing fragment from the S-layer glycoprotein of parent strain cells grown in high-salt medium modified by the low-salt tetrasaccharide was detected. (Inset) LC-ESI MS analysis of the low-salt tetrasaccharide-modified C_{55} and C_{60} dolichol phosphates in a total lipid extract of parent strain cells. (B) In Δ*aglI* cells, low-salt tetrasaccharide attached to Asn-498 is detected (lower). (Inset) LC-ESI MS analysis of a total lipid extract from Δ*aglI* cells reveals low-salt tetrasaccharide attached to C_{55} and C_{60} dolichol phosphates. The DolP-associated peaks shown in each upper panel correspond to $[M\text{-}2H]^{2-}$ ions, while Asn-498 peptide-associated peaks shown in each lower panel correspond to $[M + 2H]^{2+}$ ions. In each case, the lipid- or peptide-linked low-salt tetrasaccharide is schematically depicted at the indicated expected or observed position, with the open circle corresponding to rhamnose and the filled circles corresponding to hexose.

ating the translocation of low-salt tetrasaccharide-charged DolP across the membrane. Accordingly, Agl15 shares 28% identity and 51% similarity with AglR, recently proposed to serve as (or to assist) the flippase of DolP-mannose during the assembly of the pentasaccharide added to S-layer glycoprotein Asn-13 and Asn-83 (22).

Presently, one can only speculate on why the *Hfx. volcanii* S-layer glycoprotein is modified by the two distinct N-linked glycans under low-salt conditions but not at elevated salinity. While RNA encoding Agl5 to Agl15 was detected in cells grown at both salt levels, quantitative PCR-based studies will be necessary to determine whether comparable levels of these mRNAs are present at the different salinities. A salt concentration-related conformational change in the S-layer glycoprotein leading to exposure of Asn-498 to the low-salt tetrasaccharide N-glycosylation machinery only at the lower salinity could be imagined. The fact that this position is not modified by the Asn-13/Asn-83-linked pentasaccharide when the cells are grown at higher salinity supports this hypothesis. However, the observation that barely detectable amounts of low-salt tetrasaccharide-bound DolP are seen under high-salt conditions argues that modification of Asn-498 is a question of the availability of this glycan for transfer to this S-layer glycoprotein residue. Why cells lacking different components of the N-linked pentasaccharide biosynthetic pathway decorate Asn-

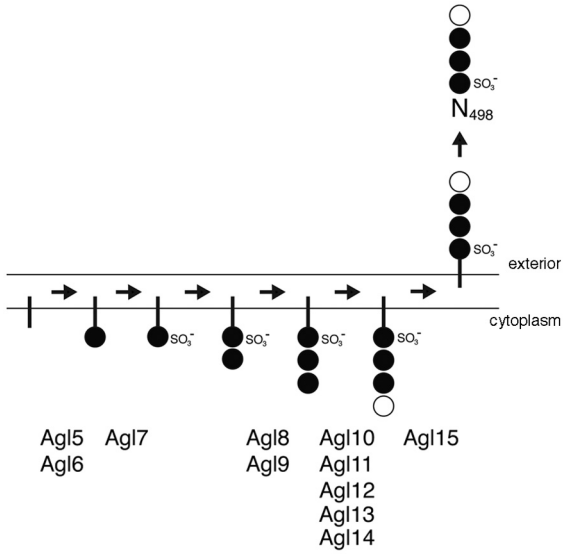

FIG 5 Working model of the assembly of the low-salt tetrasaccharide decorating S-layer glycoprotein Asn-498 in *Hfx. volcanii* cells grown in 1.75 M NaCl. The sites of action of the novel Agl proteins identified in this study are depicted. In the pathway, the vertical line corresponds to DolP, the full circles correspond to hexose, and the open circle corresponds to rhamnose. The Agl proteins listed act at the cytosolic face of the plasma membrane.

498 with the low-salt tetrasaccharide at elevated salinity also awaits explanation.

In conclusion, this study has identified components of a second *Hfx. volcanii* N-glycosylation pathway involved in the post-translational modification of the S-layer glycoprotein. Indeed, except for the *Hbt. salinarum* S-layer glycoprotein, such dual N-glycosylation of the same protein has not been reported elsewhere. While it has been shown that the variant surface glycoprotein of the eukaryotic parasite *Trypanosoma brucei* can present two distinct N-linked glycans, the compositions of the two oligosaccharides are very similar (mannose$_5$*N*-acetylglucosmine$_2$ and mannose$_9$*N*-acetylglucosmine$_2$), both relying on the same linking sugars. Moreover, both are added by isoforms of Stt3 (34, 35). Thus, the finding that AglB is not the OST of the novel *Hfx. volcanii* N-glycosylation pathway is striking. As such, an enzyme not belonging to the Stt3/PglB/AglB family of OSTs is apparently capable of catalyzing the transfer of a lipid-linked glycan to a protein target. Future efforts will need to identify this protein, as well as to address other questions, including those related to the regulation of this novel N-glycosylation pathway, as well as its interplay with the previously described *Hfx. volcanii* N-glycosylation pathway involved in adding a pentasaccharide to select Asn residues of the S-layer glycoprotein.

MATERIALS AND METHODS

Strains and growth conditions. *Hfx. volcanii* H53 parent strain cells (29) or the same cells deleted of *aglB*, *aglE*, or *aglI* (13, 15, 16, 29) were grown in medium containing 3.4 M NaCl (high salt) or 1.75 M NaCl (low salt), 0.15 M $MgSO_4{\cdot}7H_2O$, 1 mM $MnCl_2$, 4 mM KCl, 3 mM $CaCl_2$, 0.3% (wt/vol) yeast extract, 0.5% (wt/vol) tryptone, and 50 mM Tris-HCl, pH 7.2, at 42° C (36).

Quantitative PCR. Quantitative PCR was performed using Fast SYBR green master mix (Applied Biosystems, Foster City, CA). Primers (listed in Table S2) were designed using Primer Express 3.0 software (PerkinElmer Life Sciences) and employed at a final concentration of 500 nM. For PCR amplification, 10-μl reaction mixtures were subjected to 40 reaction cycles in a StepOne real-time PCR system (Applied Biosystems). Primer efficiency was ascertained by drawing a standard curve based on 4-fold serial dilutions of cDNA when primers for *HVO_2058* and *_2048* were used and 10-fold serial dilutions when primers for 16S rRNA were used. For expression analysis of *HVO_2058* and *_2048* in *Hfx. volcanii* H53 cells grown in medium containing 3.4 M or 1.75 M NaCl, 40 ng of cDNA was used in 10-μl PCR amplifications. For measuring the levels of the 16S rRNA housekeeping gene, 5 pg of cDNA was used in a 10-μl reaction mixture. Relative mRNA levels were quantified using the standard $2^{-\Delta\Delta CT}$ formula.

Gene deletion. Deletion of *Hfx. volcanii* genes of interest was achieved using a previously described "pop-in/pop-out" approach (29, 31). To amplify approximately 500-bp-long regions flanking the coding sequences of the various genes, appropriate primers directed against the upstream flanking regions and designed to introduce *Xho*I or *Kpn*I and *Hind*III sites, and against the downstream flanking regions and designed to introduce *Bam*HI and *Xba*I sites at the 5′ and 3′ of each fragment, respectively, were employed (Table S2). To confirm gene deletion at the DNA level, PCR amplification was performed using a primer directed against the upstream flanking region of the gene targeted for deletion, together with reverse primers against internal sequences of the gene in question or *trpA*, as appropriate (Table S2).

Complementation of the Δ*HVO_2058* strain was achieved upon transformation with plasmid pWL-CBD2058, encoding HVO_2058 bearing an N-terminal *C. thermocellum* cellulose-binding domain tag. DNA encoding HVO_2058, bearing introduced NdeI and KpnI restriction sites at the 5′ and 3′ ends, respectively, was ligated into plasmid pWL-CBD-AglD (19) using T4 DNA ligase (Promega), following excision of the AglD-encoding region using NdeI and KpnI. To detect the presence of *HVO_2058* in the transformed cells, PCR amplification was performed using appropriate primers (Table S2).

Mass spectrometry. LC-ESI tandem MS analysis of a total *Hfx. volcanii* lipid extract was performed as described by Kaminski et al. (18), while LC-ESI tandem MS analysis of the S-layer glycoprotein was performed as described by Guan et al. (17).

SUPPLEMENTAL MATERIAL

Supplemental material for this article may be found at http://mbio.asm.org/lookup/suppl/doi:10.1128/mBio.00716-13/-/DCSupplemental.

Figure S1, PDF file, 0.5 MB.
Figure S2, PDF file, 1.3 MB.
Figure S3, PDF file, 0.3 MB.
Figure S4, PDF file, 2.4 MB.
Figure S5, PDF file, 0.3 MB.
Figure S6, PDF file, 0.3 MB.
Table S1, DOCX file, 0.1 MB.
Table S2, DOCX file, 0.1 MB.

ACKNOWLEDGMENTS

J.E. is supported by the Israel Science Foundation (grant 8/11) and the U.S. Army Research Office (grant W911NF-11-1-520). The mass spectrometry facility in the Department of Biochemistry of the Duke University Medical Center and Z.G. are supported by Lipid Maps Large Scale Collaborative grant GM-069338 from the NIH. L.K. is the recipient of a Negev-Zin Associates Scholarship.

REFERENCES

1. **Weerapana E, Imperiali B.** 2006. Asparagine-linked protein glycosylation: from eukaryotic to prokaryotic systems. Glycobiology **16:** 91R–101R.
2. **Abu-Qarn M, Eichler J, Sharon N.** 2008. Not just for Eukarya anymore: protein-glycosylation in Bacteria and Archaea. Curr. Opin. Struct. Biol. **18:**544–550.
3. **Dell A, Galadari A, Sastre F, Hitchen P.** 2010. Similarities and differences in the glycosylation mechanisms in prokaryotes and eukaryotes. Int. J. Microbiol. 2010:. PubMed148178.
4. **Schwarz F, Aebi M.** 2011. Mechanisms and principles of N-linked protein glycosylation. Curr. Opin. Struct. Biol. **21:**576–582.
5. **Eichler J.** 2013. Extreme sweetness: protein glycosylation in Archaea. Nat. Rev. Microbiol. **11:**151–156.
6. **Kaminski L, Lurie-Weinberger MN, Allers T, Gophna U, Eichler J.** 2013. Phylogenetic- and genome-derived insight into the evolutionary history of N-glycosylation in Archaea. Mol. Phylogenet. Evol. **67:**327–339.
7. **Chaban B, Voisin S, Kelly J, Logan SM, Jarrell KF.** 2006. Identification of genes involved in the biosynthesis and attachment of *Methanococcus voltae* N-linked glycans: insight into N-linked glycosylation pathways in Archaea. Mol. Microbiol. **61:**259–268.
8. **VanDyke DJ, Wu J, Logan SM, Kelly JF, Mizuno S, Aizawa S, Jarrell KF.** 2009. Identification of genes involved in the assembly and attachment of a novel flagellin N-linked tetrasaccharide important for motility in the archaeon *Methanococcus maripaludis*. Mol. Microbiol. **72:**633–644.
9. **Maita N, Nyirenda J, Igura M, Kamishikiryo J, Kohda D.** 2010. Comparative structural biology of eubacterial and archaeal oligosaccharyltransferases. J. Biol. Chem. **285:**4941–4950.
10. **Meyer BH, Zolghadr B, Peyfoon E, Pabst M, Panico M, Morris HR, Messner P, Schäffer C, Dell A, Albers SV.** 2011. Sulfoquinovose synthase—an important enzyme in the N-glycosylation pathway of *Sulfolobus acidocaldarius*. Mol. Microbiol. **82:**1150–1163.
11. **Jones GM, Wu J, Ding Y, Uchida K, Aizawa S, Robotham A, Logan SM, Kelly J., Jarrell KF.** 2012. Identification of genes involved in the acetamidino group modification of the flagellin N-linked glycan of *Methanococcus maripaludis*. J. Bacteriol. **194:**2693–2702.
12. **Matsumoto S, Igura M, Nyirenda J, Matsumoto M, Yuzawa S, Noda N, Inagaki F, Kohda D.** 2012. Crystal structure of the C-terminal globulari domain of oligosaccharyltransferase from *Archaeoglobus fulgidus* at 1.75-Å resolution. Biochemistry **51:**4157–4166.
13. **Abu-Qarn M, Yurist-Doutsch S, Giordano A, Trauner A, Morris HR,**

Hitchen P, Medalia O, Dell A, Eichler J. 2007. *Haloferax volcanii* AglB and AglD are involved in N-glycosylation of the S-layer glycoprotein and proper assembly of the surface layer. J. Mol. Biol. **374:**1224–1236.
14. **Magidovich H, Yurist-Doutsch S, Konrad Z, Ventura VV, Dell A, Hitchen PG, Eichler J.** 2010. AglP is a S-adenosyl-L-methionine-dependent methyltransferase that participates in the N-glycosylation pathway of *Haloferax volcanii*. Mol. Microbiol. **76:**190–199.
15. **Abu-Qarn M, Giordano A, Battaglia F, Trauner A, Hitchen PG, Morris HR, Dell A, Eichler J.** 2008. Identification of AglE, a second glycosyltransferase involved in N-glycosylation of the *Haloferax volcanii* S-layer glycoprotein. J. Bacteriol. **190:**3140–3146.
16. **Yurist-Doutsch S, Abu-Qarn M, Battaglia F, Morris HR, Hitchen PG, Dell A, Eichler J.** 2008. *aglF*, *aglG* and *aglI*, novel members of a gene cluster involved in the N-glycosylation of the *Haloferax volcanii* S-layer glycoprotein. Mol. Microbiol. **69:**1234–1245.
17. **Guan Z, Naparstek S, Kaminski L, Konrad Z, Eichler J.** 2010. Distinct glycan-charged phosphodolichol carriers are required for the assembly of the pentasaccharide N-linked to the *Haloferax volcanii* S-layer glycoprotein. Mol. Microbiol. **78:**1294–1303.
18. **Kaminski L, Abu-Qarn M, Guan Z, Naparstek S, Ventura VV, Raetz CR, Hitchen PG, Dell A, Eichler J.** 2010. AglJ adds the first sugar of the N-linked pentasaccharide decorating the *Haloferax volcanii* S-layer glycoprotein. J. Bacteriol. **192:**5572–5579.
19. **Plavner N, Eichler J.** 2008. Defining the topology of the N-glycosylation pathway in the halophilic archaeon *Haloferax volcanii*. J. Bacteriol. **190:**8045–8052.
20. **Calo D, Guan Z, Naparstek S, Eichler J.** 2011. Different routes to the same ending: comparing the N-glycosylation processes of *Haloferax volcanii* and *Haloarcula marismortui*, two halophilic archaea from the Dead Sea. Mol. Microbiol. **81:**1166–1177.
21. **Cohen-Rosenzweig C, Yurist-Doutsch S, Eichler J.** 2012. AglS, a novel component of the *Haloferax volcanii* N-glycosylation pathway, is a dolichol phosphate-mannose mannosyltransferase. J. Bacteriol. **194:**6909–6916.
22. **Kaminski L, Guan Z, Abu-Qarn M, Konrad Z, Eichler J.** 2012. AglR is required for addition of the final mannose residue of the N-linked glycan decorating the *Haloferax volcanii* S-layer glycoprotein. Biochim. Biophys. Acta **1820:**1664–1670.
23. **Yurist-Doutsch S, Magidovich H, Ventura VV, Hitchen PG, Dell A, Eichler J.** 2010. N-glycosylation in Archaea: on the coordinated actions of *Haloferax volcanii* AglF and AglM. Mol. Microbiol. **75:**1047–1058.
24. **Mullakhanbhai MF, Larsen H.** 1975. Halobacterium volcanii spec. nov., a Dead Sea halobacterium with a moderate salt requirement. Arch. Microbiol. **104:**207–214.
25. **Guan Z, Naparstek S, Calo D, Eichler J.** 2012. Protein glycosylation as an adaptive response in Archaea: growth at different salt concentrations leads to alterations in *Haloferax volcanii* S-layer glycoprotein N-glycosylation. Environ. Microbiol. **14:**743–753.
26. **Lechner J, Wieland F.** 1989. Structure and biosynthesis of prokaryotic glycoproteins. Annu. Rev. Biochem. **58:**173–194.
27. **Yurist-Doutsch S, Eichler J.** 2009. Manual annotation, transcriptional analysis and protein expression studies reveal novel genes in the *agl* cluster responsible for N-glycosylation in the halophilic archaeon *Haloferax volcanii*. J. Bacteriol. **191:**3068–3075.
28. **Hartman AL, Norais C, Badger JH, Delmas S, Haldenby S, Madupu R, Robinson J, Khouri H, Ren Q, Lowe TM, Maupin-Furlow J, Pohlschroder M, Daniels C, Pfeiffer F, Allers T, Eisen JA.** 2010. The complete genome sequence of *Haloferax volcanii* DS2, a model archaeon. PLoS One **5:**e9605. doi:10.1371/journal.pone.0009605.
29. **Allers T, Ngo HP, Mevarech M, Lloyd RG.** 2004. Development of additional selectable markers for the halophilic archaeon *Haloferax volcanii* based on the *leuB* and *trpA* genes. Appl. Environ. Microbiol. **70:**943–953.
30. **Eichler J, Jarrell KF, Albers S.** 2013. A proposal for the naming of N-glycosylation pathway components in Archaea. Glycobiology **23:**620–621.
31. **Abu-Qarn M, Eichler J.** 2006. Protein N-glycosylation in Archaea: defining *Haloferax volcanii* genes involved in S-layer glycoprotein glycosylation. Mol. Microbiol. **61:**511–525.
32. **Magidovich H, Eichler J.** 2009. Glycosyltransferases and oligosaccharyltransferases in Archaea: putative components of the N-glycosylation pathway in the third domain of life. FEMS Microbiol. Lett. **300:**122–130.
33. **Wieland F, Dompert W, Bernhardt G, Sumper M.** 1980. Halobacterial glycoprotein saccharides contain covalently linked sulphate. FEBS Lett. **120:**110–114.
34. **Izquierdo L, Schulz BL, Rodrigues JA, Güther ML, Procter JB, Barton GJ, Aebi M, Ferguson MA.** 2009. Distinct donor and acceptor specificities of *Trypanosoma brucei* oligosaccharyltransferases. EMBO J. **28:**2650–2661.
35. **Izquierdo L, Mehlert A, Ferguson MA.** 2012. The lipid-linked oligosaccharide donor specificities of *Trypanosoma brucei* oligosaccharyltransferases. Glycobiology **22:**696–703.
36. **Mevarech M, Werczberger R.** 1985. Genetic transfer in *Halobacterium volcanii*. J. Bacteriol. **162:**461–462.